ASEAN Engineering Journal

Full Paper

# HYDROGEN PRODUCTION FROM WATER ELECTROLYSIS CURRENT PRACTICE VS SUSTAINABLE ALTERNATIVES

Mohammed Abdul Hannan[a], Vincent Lim Zheng Dao[a], Yaseen Adnan Ahmed[b]*, Mohd Azmi Hj Shamsuri[a]

[a]The Faculty of Science, Agriculture & Engineering, Newcastle University, UK (Singapore Campus), Singapore
[b]School of Mechanical Engineering, Faculty of Engineering, Universiti Teknologi Malaysia,81310 UTM Johor Bahru, Malaysia

**Article history**
Received
14 April 2022
Received in revised form
16 October 2022
Accepted
17 October 2022
Published online
31 August 2022

*Corresponding author
yaseen@mail.fkm.utm.my

**Graphical abstract**

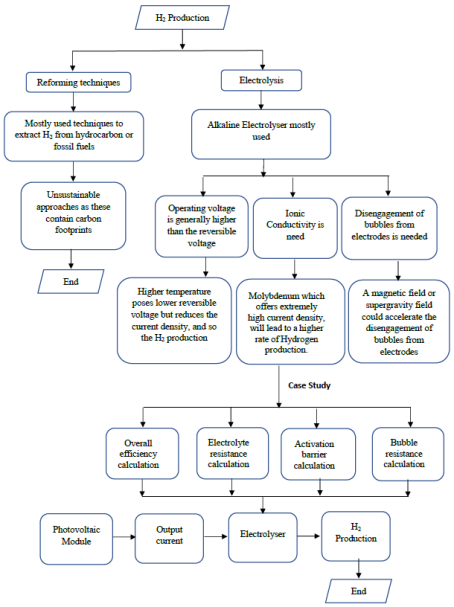


## Abstract

Research and development on sustainable alternatives to fossil fuels have become a prime focus for the last couple of decades. Hydrogen, one of Earth's most abundant elements, holds great potential as a sustainable energy carrier. However, as Hydrogen is lighter than air, it does not exist in pure form in the atmosphere and is often found in compounds, such as water. The abundance of seawater in this regard makes Hydrogen an almost inexhaustible source of energy. Nevertheless, sustainable ways of extracting Hydrogen from water, dealing with its high corrosiveness and significantly lower evaporation point, still pose research challenges. Therefore, this paper aims at providing a comprehensive analysis of sustainable Hydrogen generation by focussing on the application of electrolysis to recover Hydrogen from water rather than using common reforming techniques. Different parameters affecting the efficiency and the overall performance of the electrolyser process have also been discussed and possible solutions to tackle the problems are presented. Later, a case study has been conducted to demonstrate the sustainable alternative for hydrogen production for an alkaline electrolyser using solar energy. MATLAB Simulink platform is used in this regard. This paper concludes that at an irradiation level of 1000W/m2, a PV array with 57 parallel strings with four modules connected in series per string is sufficient to provide enough power for the electrolyser to produce Hydrogen.

*Keywords*: Hydrogen production, Photovoltaic, Alkaline Electrolysis, MATLAB-SIMULINK, Solar



## 1.0 INTRODUCTION

Greenhouse gases and global warming have become a burning issue in recent years due to their prominent impacts on our environment. As the burning of fossil fuel is the main source of such harmful gases, searching for a cleaner fuel has revealed the possibility of harnessing Hydrogen as an energy carrier among other alternatives such as LNG, methanol, and ammonia. However, the advantage of Hydrogen over other alternatives is that it offers potentially zero carbon emissions, removes the issue of unburnt hydrocarbons, with water being its only by-product. A major drawback of Hydrogen, on the other hand, is that with an evaporation point of 20.25K/~-253°C, the storage of liquid Hydrogen requires specialized insulation materials or pressurizing the storage tank to prevent evaporation. Besides, it must be produced since it does not exist in its free state naturally; therefore, energy input is required to extract pure Hydrogen to use as fuel.

Two common methods of producing Hydrogen these days are processing fossil fuels (most Hydrogen produced this way) and electrolysis. The three technologies that are commonly used to extract Hydrogen from fossil fuels or hydrocarbons are Steam Methane Reforming (SMR), Partial Oxidation (POX) and Auto-Thermal Reforming (ATR). The principle of reforming is the production of synthesis gas (syngas), a mixture gas comprising of Hydrogen, Carbon Monoxide and Carbon Dioxide. Syngas can be produced from almost any hydrocarbon feedstock, such as coal and natural gas. Among these three, SMR is the most dominant method where methane is mixed

with steam to produce carbon dioxide and Hydrogen as shown in Equation 1.

$$CH_4 + 2H_2O \rightarrow CO_2 + 4H_2 \quad (1)$$

This endothermic reaction produces a high H2/CO ratio of approximately 3:1. Due to this high ratio, SMR has remained to be the most used method in Hydrogen production. However, this endothermic reaction often promotes carbon or coke formation. Though, use of Group VIII noble metals as catalyst seem to minimize coke formation [1]. While SMR does produce the highest yield of Hydrogen between the three technology, it also produces about 13.7 kg CO2 per kg yield of H2 [2]. Thus, it will be ironic to produce clean Hydrogen fuel when the reforming process generates such an amount of pollutants.

POX, on the other hand, is an exothermic reaction that uses methane and limited oxygen instead of steam, to produce syngas as shown in Equation 2.

$$CH_4 + 1/2O_2 \rightarrow CO + 2H_2 \quad (2)$$

Since this process is exothermic, the heat generated could be used in an endothermic process such as SMR, which can make POX much more energy efficient. Another advantage of POX is that it does not require the addition of heat such as superheated steam like SMR, which helps cuts down on the capital cost to generate steam. However, an oxygen separation plant may be needed to separate nitrogen in the air which is undesirable in pressurized down-stream processes [3]. Processing temperatures of up to >1000°C are required to reduce soot formation, but it is difficult to control the temperature in an exothermic reaction. The yield of H2 is also significantly lower than that produced from SMR.

The third method, ATR is a combination of both SMR and POX. It involves the heat generated from POX and incorporating that heat energy to an endothermic process such as SMR. This process eliminates the need to provide an external heat source but creates problems, such as carbon formation and the need for costly oxygen separator, similar to the POX process. The formation of carbon or soot can cause damage to equipment and create heat transfer issues [4].

Although Hydrocarbon reforming methods have proved highly efficient and cost-effective due to the extensive industrial experience, they emit a great amount of greenhouse gas. Therefore, it is crucial to emphasis on other non-reforming methods of Hydrogen production to tackle sustainability issues. One such promising method is Electrolysis, which is simply the process of splitting Hydrogen and oxygen molecules in water by passing electricity through two electrodes. There are three main types of electrolysers used in Hydrogen production: Alkaline Electrolyser being the most common, Proton Exchange Membrane (PEM) electrolyser and Solid Oxide Electrolysis Cells (SOEC) units [1]. Electrolysis has been proven to produce Hydrogen of high purity, and the technology is also well established [5]. However, the amount of Hydrogen produced by electrolysis is often not enough or economical to meet large-scale industrial consumption [6].

This research, therefore, aims at performing a comprehensive analysis of Alkaline Electrolyser, the mostly adopted non-reforming methods of Hydrogen production from non-hydrocarbon sources. Followed by highlighting the effect of different system parameters on the efficiency and overall performance of the alkaline electrolyser process and proposing a few possible solutions to boost the efficiency. A case study of alkaline electrolyser is also carried out to demonstrate the success of sustainable alternative for hydrogen production using solar energy, where a theoretical model of Photovoltaic Modules (PV) is analysed to provide the electricity needed for Hydrogen production. The overall framework of this research study is presented in Figure 1.

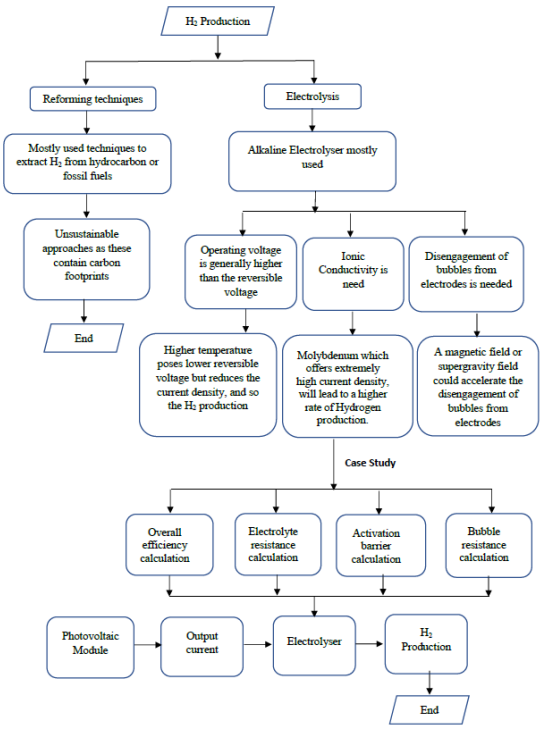


**Figure 1.** Framework of the work process

Following the introduction, the basics of Alkaline Electrolyser is presented next. After that, techniques for increasing Hydrogen production, for example, reducing the reversable voltage, increasing ionic conductivity and accelerating the disengagement of bubbles from electrodes are discussed. Finally, the methodologies for incorporating the renewable energy sources for sustainable hydrogen production are presented, followed by the results obtained from the case study.

## 2.0 ALKALINE ELECTROLYSER

Alkaline electrolyser provides the advantage of simplicity, also the most matured electrolysis technology proven in the industry, offering lower CAPEX and OPEX for Hydrogen production. Both PEM and alkaline electrolyser are undergoing intensive R&D to optimise their efficiency in providing grid services when coupled either directly or indirectly to Renewable Energy Sources (RES) [7]. Figure 2 shows the schematic diagram of a basic electrolysis system.

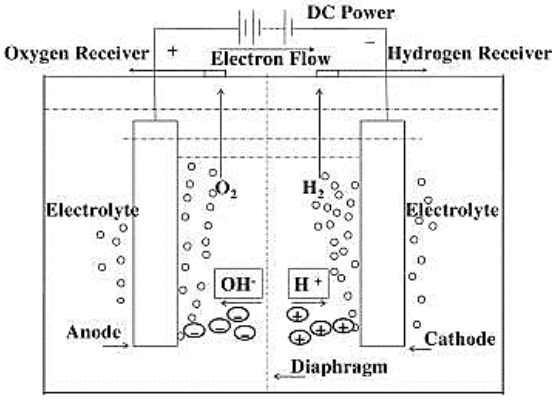


**Figure 2.** Schematic Diagram of Electrolysis [6]

The chemical reactions occurring at both cathode and anode of this system are:

$$\text{Cathode: } H_2O+2e^- \rightarrow H_2+2OH^- \quad (3)$$

$$Anode: 2OH^- \rightarrow \frac{1}{2}O_2+H_2O+2e^- \quad (4)$$

Here, an input voltage is required to break water into its elements. The minimum voltage or reversible voltage (VRev) required at room temperature, and 1 atm pressure is:

$$V_{REV} = \frac{-\Delta G}{nF} = \frac{-(-237.2*10^3)}{2*96486} = 1.23\text{V} \quad (5)$$

Where ΔG is the standard Gibbs free energy for the formation of water, n is the number of moles, and F is the Faraday constant.

However, the operating voltage is generally higher than the reversible voltage due to resistances in the system, such as ohmic resistance from the electrolyte, overpotentials at the cathode and anode, transportation, and charge transfer [8]. Industrial electrolyser usually operates at a range of 1.8-2.0 V [9]. The operating voltage, VOper, is calculated using Equation 6.

$$V_{Oper} = V_{Rev}+\Sigma\eta+iR_{Cell} \quad (6)$$

Where $\eta$ is the overpotentials required to overcome the energy barrier at both anode and cathode. Tafel equation as shown in Equation 7 is usually used to calculate this parameter.

$$\eta = a + b\,logi \quad (7)$$

*a* and *b* here are Tafel constants that are dependent on the properties of the electrode material, and *i* is the current density given by the division of current over the electrode surface area. Hence, the summation of $\eta$ is given as:

$$\Sigma\eta = |\eta_{Cathode}|+|\eta_{Anode}| \quad (8)$$

$iR_{Cell}$ in Equation 6 is given as the total ohmic voltage drop across the system due to resistances that is discussed later in this paper.

Any component within an electrical circuit provides resistances. Ohmic losses in electrolysis are not preventable but can be minimised by optimising the design of electrodes, choice and quality of electrolyte, cell designs or configurations, etc. Membrane resistance (Rm), bubble formation (Rb), electrolyte resistance (Re) and total circuit resistance (Rc) contributes to the total ohmic losses of the entire electrolysis process as shown in Equation 9, which in turn, requires a higher voltage to drive the separation of water into Hydrogen and oxygen.

$$\Sigma R = R_e+R_m+R_b+R_c \quad (9)$$

## 3.0 IMPROVING ALKALINE ELECTROLYSER PROCESS FOR SUSTAINABLE HYDROGEN PRODUCTION

### Voltage Reduction

The operating voltage for the electrolysis process can be reduced if any of the three voltages on the RHS of Equation 6 can be decreased. The reversible or equilibrium voltage can be decreased below 1.23V, as shown in Figure 3 if the temperature is increased. The thermoneutral voltage denoted in this diagram is the minimum operating voltage of the system.

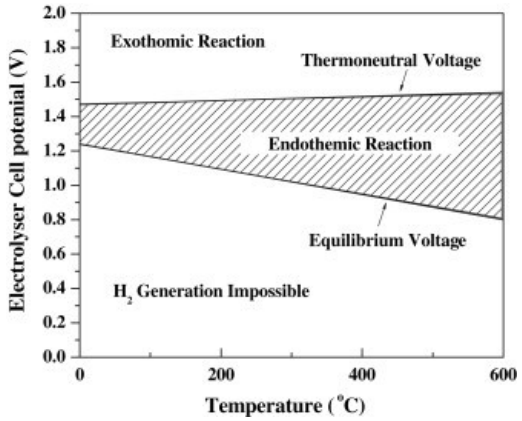


**Figure 3.** Cell Potential as a function of temperature [6]

From Figure 3, we can see that by conducting electrolysis in a high-temperature setting, it is possible that we could lower the reversible voltage. However, higher operating temperature poses other problems, such as an extremely quick electrolyte evaporation rate. Higher quality of materials will also be required to withstand high operating temperatures, and a reduction in current density due to the lowered voltage directly diminishes the rate of Hydrogen production.

Overpotentials at the electrodes depend on the electrode material as well as on the effective area. Choice of electrodes also depends on but is not limited to electrochemical stability, electrical conductibility, and high corrosion resistance. Platinum and Palladium as electrodes show low overpotentials, whereas Zinc and Lead show high overpotentials. However, due to the high cost of platinum and Palladium, most electrodes conform to middle overpotentials such as Nickel based metals or alloys [10] which provides a balance between cost and compatibility. Apart from the voltage issue, high electrical resistance in the circuit results in energy loss through heat generation. This leads to high energy consumption while sub

utilising the power provided. Electrical resistances in the circuit mostly originate from wire connections, ions conductivity in the electrolyte, bubble formation at electrodes, and distance between both cathode and anode.

**Ionic Conductivity**

Pure water cannot be utilised effectively in electrolysis due to its poor ionic conductivity, so acids or bases are used as additives to enhance ionic conductivity. 25-30% potassium hydroxide (KOH) is used extensively in an alkaline electrolyser [11]. In some cases, sodium hydroxide (NaOH) or sulphuric acid ($H_2SO_4$) also acts as conductive salts [12]. However, the corrosive nature of both alkali and acid poses a challenge to the degradation of materials in the system, and metal electrodes lose their catalytic activity in a short span of time. Ionic liquids (salts that are in a liquid state at room temperature) are introduced to mitigate the situation. For example, Souza et al. [13] experimented with the use of 1-butyl-3-methyl-imidazolium-tetrafluoroborate ($BMIBF_4$) and showed that the solution is chemically inert to metal electrodes but exhibited great ionic conductivity. Table 1 shows the performance of the different types of metallic electrodes in the presence of $BMIBF_4$. As noticed, all electrodes perform at higher efficiency, especially molybdenum offering an extremely high current density, *J*, which in turn, will lead to a higher rate of Hydrogen production.

**Table 1.** Electrochemical Performance of different metallic electrodes [13]

| Electrode | Cathodic Limit (V) | Anodic Limit (V) | J (mA/cm$^2$) | Q/S (C/cm$^2$) | h (%) |
|---|---|---|---|---|---|
| Ni | -2.0 | 2.1 | 14.6 | 71.9 | 99.1 |
| $FeCr_4$ | -2.1 | 0.4 | 19.8 | 86.7 | 99.0 |
| $FeCr_8$ | -1.7 | 1.1 | 22.6 | 89.9 | 99.2 |
| $FeMn_{12}$ | -2.1 | 0.6 | 23.0 | 76.8 | 97.6 |
| $Ni_{77}$ | -2.4 | 2.6 | 31.0 | 98.5 | 94.6 |
| Mo | -1.8 | 1.8 | 77.5 | 301.0 | 99.2 |

**Bubble Formation**

As the electrolysis process goes on, Hydrogen and oxygen bubbles begin to form on the respective electrodes. Over time, ideally, these bubbles should grow into the critical size and leave the electrode's surface as soon as possible as they are covering active areas for Hydrogen generation. However, in reality, the bubbles remain on the electrodes during nucleation and growth, thus reducing the active areas. This event leads to high ohmic voltage drop and high overpotentials, which further increases the total resistance in electrolysis. The diameter of the bubbles was observed to be related to current density and pressure. The higher the diameter, the higher the current density and the lower the pressure [14]. Formation of these bubbles not only occur on the electrodes, but also in membrane, and the distance between each electrode greatly impacts the overall resistance in the electrolyte, $R_e$ which is calculated using Equation 10.

$$R_e = \frac{\rho l}{A} = \frac{\rho}{A}\sum l_i \quad (10)$$

Here $\rho$ is the material resistivity, *A* is the cross-sectional area, and *l* is the coverage of the electrolyte, or distance between the electrode in a conventional setup.

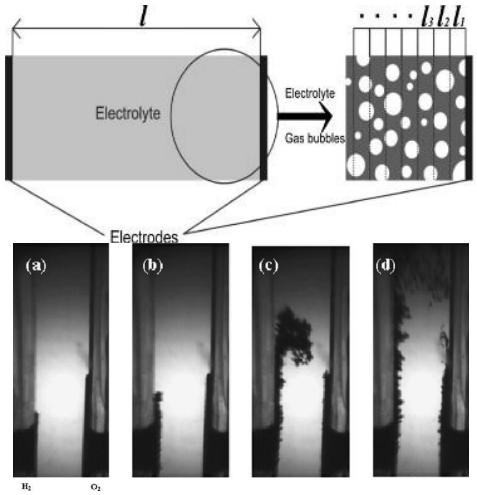


**Figure 4. (a)** Up: Void fraction formation [15], and **(b)** Down: Bubble Layer [16]

Figure 4(a) shows the distance between electrodes broken into smaller divisions "*li*". It should be noted that the bubble formation reduces the effective cross-sectional area for individual *li*, thus increasing the overall resistance in the electrolyte [15]. Figure 4(b) shows the slow bubble disengagement resulted in the formation of a bubble curtain, and the thickness increases with electrode height [16]. Various strategies have been applied to accelerate the disengagement of bubbles from electrodes by an external field, such as introducing a magnetic field or supergravity field [12].

**Incorporating renewable Energy**

The drawback of electrolysis has always been the high energy consumption and the source of this energy, being from fossil fuels, seems to offset the advantage of Hydrogen being used as a zero-emission fuel. PV modules can be coupled to an electrolyser to provide the needed electricity for water splitting, as electrolyser can generally perform in a stable condition despite a fluctuating energy source [17]. A recent study [18] shows that unused solar power amounts to more than $7*10^6$ kWh in China out of the total produced PV power of 28.7 billion kWh, akin to about 20% wastage. Similar trends can be observed in Australia and many European countries these days. Therefore, the benefits of coupling solar energy with electrolyser will be twofold – reducing solar power wastage and producing Hydrogen sustainably.

*PV-Electrolyser*

A conventional setup of PV modules connecting to an electrolyser using DC/DC converters and storage batteries is shown in Figure 5. The purpose of the batteries is to provide the stored energy captured from the PV cells to the electrolyser during times of low solar irradiation, such as night-time, monsoon or winter seasons. DC/DC converters or Maximum Power Point Tracker (MPPT) serves as a major component in PV-Electrolysis to regulate the output power of the PV modules to match with the electrolyser operating power, assuring

maximum efficiency is achieved from the overall system. Another type of configuration would be to couple both PV modules and grid electricity to an electrolyser to ensure a constant supply of electricity for Hydrogen production. This again eliminates any fluctuating source of power due to diurnal variations and provides a more reliable source of power compared to batteries due to batteries' limited capacity.

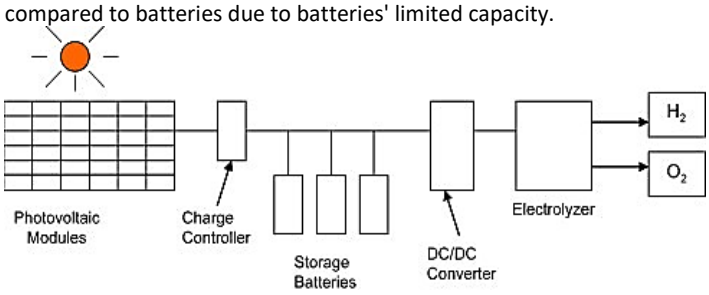


**Figure 5.** Conventional PV electrolyser [19]

## 4.0 METHODOLOGY

The theoretical background behind the case study is presented in this section which demonstrates the impact of various resistances on the net voltage required for electrolysis. This study is subjected to the following assumptions:

- Electrolysis is carried out at 298K atm, and the electrolyte used will be 30% w.t KOH.
- Both cathode and anode are of exact dimensions of 10cm2 each, 2cm(L)*5cm(H). Area of membrane is 25cm$^2$, 5cm(L)*5cm(H)*2mm(t).
- Resistance due to membrane/separator is assumed to be inclusive in the net electrolyte resistance.
-

**Electrolyte Resistance**

The electrolyte resistance (Equation 10) depends on several conditions. Since the total area and length are considered fixed, only the material resistivity, $\rho$ needs to be calculated. The material resistivity ($\rho$) is the reciprocal of the specific conductivity, *k*, of the electrolyte as shown in Equation 11.

$$\rho = \frac{1}{k} \tag{11}$$

The specific conductivity of the electrolyte (*k*) is related to the molarity concentration of the electrolyte, as well as the temperature in Kelvin [20], which is shown in Equation 12.

$$k = A(M) + BM^2 + C\,(M \times T) + D\,(\frac{M}{T}) + EM^3 + F\,(M^2 \times T^2) \tag{12}$$

Where *k* is in S/cm, *M* is the molarity in mol/L and *T* in Kelvin. The constants A to F can be found in Table 2.

Table 2. Constants for specific conductivity calculation [27]

| Constant | A | B | C | D | E | F |
|---|---|---|---|---|---|---|
| Value | -2.041 | -0.0028 | 0.00533 | 207.2 | 0.00104 | -3.00E-07 |

To calculate the molarity of the electrolyte, the density ($\delta$) of 30% w.t KOH at 298K must be known, which can be found as:

$$\delta = \mu\, e^{(0.0086 \times w.t\%)} = 997.03\, e^{(0.0086 \times 30)} = 1290.495\ \mathrm{kg/m^3} \tag{13}$$

Where $\mu$ is a constant at 298K. Now, density and molarity are related as:

$$\delta = \mathrm{AM^2 + BM + C} \tag{14}$$

A=-0.4931, B=45.761 and C=999.63 are constants relating density to molarity at 298K [26]. Using Equation 14, the molarity of 30% w.t KOH is 6.8637 mol/L. So, the specific conductivity (*k*) for given M=6.8637 mol/L and T=298K will be 0.6198 *S/cm* (Equation 12), and the resultant material resistivity ($\rho$) will be 1.613 $\Omega.cm$ (Equation 11). Now using Equation 10, the net electrolyte resistance for varying distances of electrodes can be determined, as depicted in Figure 6. As observed, the resistance follows a linear trend.

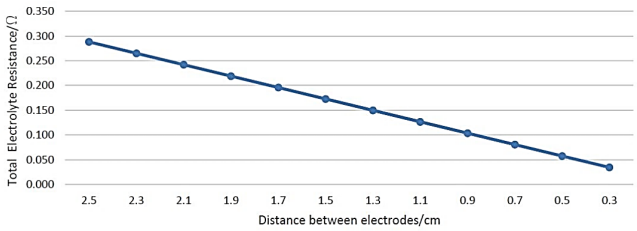


**Figure 6.** Electrolyte Resistance with varying electrode distances

Thus, to optimise the system, ideally, the zero-gap cell design, which is zero spacing between electrodes, can be employed. Practically, the closest distance achieved is 2mm between solid electrodes [21]. However, utilising porous mesh electrodes, the zero-gap cell design can also be achieved [22].

**Activation Barrier**

Another major resistance for the electrolysis system is the overpotential at the electrodes, which requires an additional voltage to overcome the activation barrier due to reaction kinetics. In an ideal situation where little or no gas bubbles are formed, the current density is given by the division of current intensity over the electrode surface area. However, in a practical situation, bubbles will be formed, covering the active surface of the electrodes and hence acts as a source of impedance. The real current density ($j_\vartheta$), considering bubble coverage, can be calculated as:

$$j_\theta = \frac{I}{A(1-\theta)} = \frac{1}{10(1-0.2)} = 0.125\ A/cm^2 \tag{15}$$

Where, *I* is the current intensity, *A* is the surface area of the electrode, and $\vartheta$ is the bubble coverage ratio, which is assumed to be 20% in this case. From Equation 8, the total activation overpotential can be calculated as follows using the Butler-Volmer Equation [23].

$$\eta_{Total} = \frac{RT}{\alpha F} In \frac{j_\theta}{i_{\theta anode}} + \frac{RT}{\alpha F} In \frac{j_\theta}{i_{\theta cathode}} = \frac{R(298)}{0.5F} In \frac{0.125}{0.016} + \frac{R(298)}{0.5F} In \frac{0.125}{0.02} = 0.2 \tag{16}$$

Where *R* is the universal gas constant, 8.314J/mol.K, *T* is the operating temperature in Kelvin, $\alpha$ is the mass transfer coefficient which lies between 0 and 1 and assumed generally

to be 0.5 for both cathode and anode. *F* is the Faraday constant at 96485C/mol.

**Bubble Resistance**

Ohmic resistance resulting from bubble formation can be calculated [24] as:

$$R_{Bubble,H_2} = \frac{L_{cathode,anode}}{A_{Tank} * k_{water} * (1 - 1.5 * V)} \quad (17)$$

Where *k* is the electrolyte specific conductivity, and *V* is the volume fraction of gas in the solution assumed at 0.1.

$$R_{Bubble,O_2} = \frac{L_{cathode,anode} * \rho_{resistivity}}{A_{Tank}} \quad (18)$$

$$\text{Where, } \rho_{resistivity} = \rho_0 (1 - \theta)^{-\frac{3}{2}} \quad (19)$$

And $\rho_0$ is the specific resistivity of the electrolyte. These Equation 17 and 18 gives 0.304Ω and 0.361Ω, respectively and summing up to 0.665Ω as total bubble resistance.

**Overall Efficiency**

The resistance from wire connections is considered negligible as a small system is assumed for this case study, and considering the distance between electrodes as 2.5 cm, electrolyte resistance is found to be 0.288Ω. Thus, combining all the resistances in the system, the operating voltage of the electrolysis process can be calculated using Equation 6 as:

$$V_{Oper} = 1.23 + 0.2 + i(0.288+0.665) = 2.38V \quad (20)$$

And the overall voltage efficiency [10] is given by:

$$\eta_{voltage} = \frac{V_{Rev}}{V_{Oper}} = \frac{1.23}{2.38} * 100\% = 51.58\% \quad (21)$$

Other efficiencies such as thermal efficiency [10] can be derived as:

$$\eta_{Thermal} = \frac{V_{Rev}}{V_{Oper}} = \frac{1.48}{2.38} * 100\% = 62.18\% \quad (22)$$

The thermoneutral voltage is 1.48V as mentioned above for water electrolysis at 298K. Hence, to show the effect of reducing electrodes distance on the overall efficiency of the system, Equation 20 can be re-evaluated with the resistance of electrolyte at 3mm distance, 0.035Ω, resulting in an operating voltage of 2.13V; thus, a voltage efficiency of 57.75%, an increase of approximately 6%. It should also be observed that the bubble resistance provides the bulk of impedance to the system.

## 5.0 RESULTS AND DISCUSSION

Following the theoretical formulation, this section discusses the results obtained, starting with the size selection for the PV array. PV arrays are formed by connecting PV modules, while solar cells are connected in series to form the PV modules. The electrolyser power requirement for a pre-determined Hydrogen production rate must be found before deciding the size of the PV array. For example, Figure 7(a) shows the operating voltage at different operating pressure and temperature, and Figure. 7(b) shows the power required for generating a pre-determined amount of Hydrogen at various pressure and temperature [25].

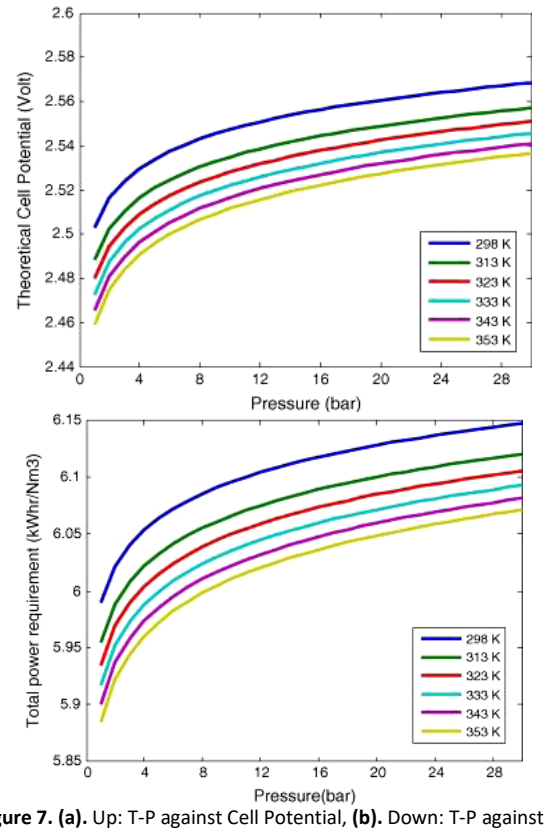


**Figure 7. (a).** Up: T-P against Cell Potential, **(b).** Down: T-P against Power.

If a 50 cells electrolyser connected in series is operating at the same temperature and pressure (298K and 1 atm) as mentioned in the previous subsection, the voltage required from the PV array will be 2.5V/cell * 50 cells, giving a total of 125V (Figure 7(a)). To generate Hydrogen at a rate of 5Nm$^3$/hr, the power required from the PV array will be 6kWh/Nm$^3$ * 5Nm$^3$/hr =30kW (Figure 7(b)). Hence, the total current output per cell required from the PV array can be found, following Watt's Law, I=P/V.

$$Current\ required = \frac{30 * 10^3}{125} = 240\ A \quad (23)$$

Table 3 shows the parameters for a typical solar cell and the electrical characteristics at Standard Test Conditions (STC), where irradiance level is 1000W/m$^2$, the spectrum air mass is 1.5, and cell temperature is 25°C. Using the data from Table 3, the solar cell is modelled in MATLAB-SIMULINK to attain its PV and IV characteristics. The five parameters, the single diode model, as reviewed by Lun et al. [26] are used for this modelling. The parameters are calculated using Equation 24-28.

**Table 3.** Characteristics of typical solar cell

| | |
|---|---|
| **Model** | Shell SP140-PC |
| **No. of Cells in series** | 72 |
| **Dimensions per Module(mm)** | 814(L)*1622(H)*40(W) |
| **Rated Power** | 140W |
| **Peak Voltage ($V_{MPP}$)** | 33V |
| **Peak Current ($I_{MPP}$)** | 4.25A |
| **Open Circuit Voltage** | 42.8V |
| **Short Circuit Current** | 4.7A |

$$I = I_{ph} - I_0 e^{\left(\frac{q.(V+I.R_S)}{n.K.N_S.T}\right)-1} - I_{sh} \quad (24)$$

Where I is the output current, $I_{ph}$ is the photocurrent, $I_0$ is the saturation current, $I_{sh}$ is the current through a shunt resistor, q is the electron charge constant at $1.6*10^{-19}$ C, $R_s$ is the series resistance, n is the ideality factor of the diode assumed at 1.3, K is the Boltzmann's constant at $1.38*10^{-23}$J/K, $N_s$ is the number of cells connected in series, and T is the operating temperature in Kelvin.

$$I_{ph} = I_{sc} + k_i.(T - T_{STC})\frac{G}{G_{STC}} \quad (25)$$

Where Isc is the short circuit current, ki is the temperature coefficient for short circuit current in A/°C, $T_{STC}$ is the temperature in Kelvin at STC, G is the received irradiance level, and $G_{STC}$ is the irradiance at STC.

$$I_o = I_{rs}.(\frac{T}{T_{STC}})^3.e^{\frac{q.E_{go}.(\frac{1}{T_{STC}}-\frac{1}{T})}{n.K}} \quad (26)$$

Where $I_{rs}$ is the reverse saturation current, $E_{go}$ is the energy gap of the materials of the cell.

$$I_{rs} = \frac{I_{sc}}{e^{\frac{q.V_{oc}}{n.N_{s.K.T}}-1}} \quad (27)$$

Where $V_{oc}$ is the open-circuit voltage.

$$I_{sh} = \frac{V + I.R_s}{R_{sh}} \quad (28)$$

Where $R_{sh}$ is the shunt resistance at 415Ω, $R_s$ is the series resistance calculated to be 0.725Ω.

The solar module using the parameters stated in Table 3 is modelled in MATLAB Simulink. After running the simulation, the PV and IV characteristics of the solar cell is obtained at different levels of irradiation as shown in Figure 8(a) and 8 (b). From the solar irradiation levels at the site, it is possible to calculate the number of PV modules needed to build the array.

Assuming the irradiation level of 1000W/m$^2$, theoretically, the number of panels required is 30000/140=214. However, as found in Figures 8(a) and 8(b), 214 panels will not be enough to meet the current and voltage needed for electrolysis. To provide enough power for the generation of 5Nm$^3$/hr, the configuration of the array has to be 57 parallel strings with four modules connected in series per string, giving 228 panels to provide a total output power of 31980W, 132V, and 242.3A. The PV array is assumed to output the corresponding power required by the electrolyser using MPPT. The resulting area necessary for only the solar panels will amount to 7.42m$^2$. Sizing of the panels and adjusting the output of the PV array to assure maximum efficiency is essential. Since most of the Hydrogen produced in the world is from methane reforming, the amount of carbon dioxide reduction by using PV or other renewable methods can be up to 7.33kg for per kg of Hydrogen produced [27].

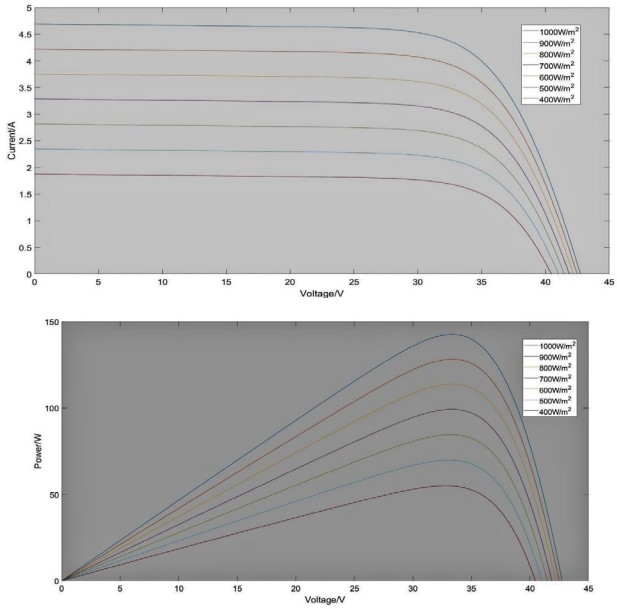


**Figure 8. (a).** Up: IV Curve at 25 deg. C for various irradiation levels, **(b).** Down: PV Curve at 25 deg. C for various irradiation levels

## 6.0 CONCLUSIONS

The recent trends in electrolysis for Hydrogen production are summarized and the drawbacks are highlighted. Following that, some techniques for efficiency improvements are described. A case study is then presented to theoretically demonstrates how Hydrogen can be produced in a sustainable way using solar as the source of energy. However, unlike the case study presented, an industrial-sized PV plant will take up more than 100 times the area that is mentioned here since the Hydrogen generation rate will be much higher in an industry setup. Nevertheless, as demonstrated it is definitely a feasible option to employ PV cells for Hydrogen generation in a sustainable way. Besides, as described optimising the design of the electrolyser will also increase the overall efficiency of the process as the PV conversion efficiency often lies between 10-20%.

## Acknowledgement

The content of this paper was submitted to Singapore Institute of Technology student repository as a part of the

partial fulfilment of NU SIT joint BEng degree requirement.

## References


[1] Dawood, F. Anda, M., and Shafiullah, G.M. 2020. Hydrogen production for energy: An overview. *International Journal of Hydrogen Energy* 45(7)

[2] Muradov, N.Z., and Veziroğlu, T.N. 2005. From hydrocarbon to Hydrogen–carbon to Hydrogen economy, *International Journal of Hydrogen Energy*, 30(3): 225-237.

[3] York, A.P., Xiao, T., and Green, M.L. 2003. Brief overview of the partial oxidation of methane to synthesis gas, *Topics in Catalysis*, 22(3-4): 345-358.

[4] Ma, R., Xu, B., and Zhang, X. 2019. Catalytic partial oxidation (CPOX) of natural gas and renewable hydrocarbons/oxygenated hydrocarbons—A review." *Catalysis Today*, 338: 18-30.

[5] Stojić, D.L., Marčeta, M.P., Sovilj, S.P., and Miljanić, Š.S. 2003. Hydrogen generation from water electrolysis—possibilities of energy saving, *Journal of Power Sources,* 118(1-2): 315-319.

[6] Kovac, A., Marcius, D., and Budin, L. 2019. Solar hydrogen production via alkaline water electrolysis. *International Journal of Hydrogen Energy*, 44(20).

[7] Matute, G., Yusta, J.M., and Correas, L.C. 2019. Techno- economic modelling of water electrolysers in the range of several MW to provide grid services while generating Hydrogen for different applications: A case study in Spain applied to mobility with FCEVs, *International journal of Hydrogen energy,* 44(33): 17431-17442.

[8] Rashid, M.M., Al Mesfer, M.K., Naseem, H. and Danish, M. 2015. Hydrogen production by water electrolysis: a review of alkaline water electrolysis, PEM water electrolysis and high temperature water electrolysis, *Int. J. Eng. Adv. Technol*, 4(3): 2249-8958.

[9] Khaselev, O., Bansal, A. and Turner, J.A. 2001. High- efficiency integrated multijunction photovoltaic/electrolysis systems for Hydrogen production, *International Journal of Hydrogen Energy,* 26(2): 127- 132.

[10] Lupi, C., Dell'Era, A., and Pasquali, M. 2009. Nickel– cobalt electrodeposited alloys for Hydrogen evolution in alkaline media, *International Journal of Hydrogen Energy,* 34(5): 2101-2106.

[11] Petrov, Y., Schosger, J.P., Stoynov, Z. and De Bruijn, F. 2011. Hydrogen evolution on nickel electrode in synthetic tap water–alkaline solution, *International journal of Hydrogen energy*, 36(20): 12715-12724.

[12] Wang, M., Wang, Z., Gong, X., and Guo, Z. 2014. The intensification technologies to water electrolysis for Hydrogen production–A review, *Renewable and Sustainable Energy Reviews*, 29: 573-588.

[13] Roberto, F.D.S., Gabriel, L., Janine, C.P., Emilse, M.A.M., and Michele, O.D.S. 2008. "Molybdenum electrodes for Hydrogen production by water electrolysis using ionic liquid electrolytes," *Electrochemistry Communications*, 10: 1673-1675.

[14] Caboussat, A., Kiss, L., Rappaz, J., Vékony, K., Perron, A., . Renaudier, S., and Martin, O. 2011. Large gas bubbles under the anodes of aluminum electrolysis cells, In Light Metals, 581-586, Springer, Cham.

[15] Mazloomi, S.K., and Sulaiman, N. 2012. Influencing factors of water electrolysis electrical efficiency, *Renewable and Sustainable Energy Reviews*, 16(6): 4257-4263.

[16] Matsushima, H., Iida, T., and Fukunaka, Y. 2012. Observation of bubble layer formed on Hydrogen and oxygen gas-evolving electrode in a magnetic field," *Journal of Solid State Electrochemistry*, 16(2): 617-623.

[17] Cox, K.E. 2018. Hydrogen from solar energy. *Hydrogen: Its Technology and Implication, Production Technology*- I (1): 145.

[18] Chi, J., and Yu, H. 2018. Water electrolysis based on renewable energy for Hydrogen production, *Chinese Journal of Catalysis,* 39(3): 390-394.

[19] Gibson, T.L, and Kelly, N.A. 2008. Optimisation of solar powered Hydrogen production using photovoltaic electrolysis devices, *International Journal of Hydrogen Energy*, 33(21): 5931-5940.

[20] Gilliam, R.J., Graydon, J.W., Kirk, D.W., and Thorpe, S.J. 2007. A review of specific conductivities of potassium hydroxide solutions for various concentrations and temperatures, *International Journal of Hydrogen Energy,* 32(3): 359-364.

[21] Sakr, I.M., Abdelsalam, A.M., and El-Askary, W.A. 2017. Effect of electrodes separator-type on hydrogen production using solar energy, *Energy*, 140: 625-632.

[22] Phillips, R., Edwards, A., Rome, B., Jones, D.R., and Dunnill, C.W. 2017. Minimising the ohmic resistance of an alkaline electrolysis cell through effective cell design, *International Journal of Hydrogen Energy*, 42(38): 23986-23994.

[23] Roy, A., Watson, S. and Infield, D. 2006. Comparison of electrical energy efficiency of atmospheric and high- pressure electrolysers, *International Journal of Hydrogen Energy*, 31(14): 1964-1979.

[24] Zouhri, K., and Lee, S.Y. 2016. Evaluation and optimisation of the alkaline water electrolysis ohmic polarisation: Exergy study, *International Journal of Hydrogen Energy*, 41(18): 7253-7263.

[25] Bhattacharyya, R., Misra, A., and Sandeep, K.C. 2017. Photovoltaic solar energy conversion for Hydrogen production by alkaline water electrolysis: conceptual design and analysis, *Energy Conversion and Management*, 133: 1-13.

[26] Lun, S.X., Du, C.J., Guo, T.T., Wang, S., Sang, J.S., and Li, J.P. 2013. A new explicit I–V model of a solar cell based on Taylor's series expansion, *Solar Energy,* 94: 221-232.

[27] Kothari, R., Buddhi, D., and Sawhney, R.L. 2008. Comparison of environmental and economic aspects of various Hydrogen production methods, *Renewable and Sustainable Energy Reviews,* 12(2): 553-563.